Syracuse University

SURFACE

9-5-2011

Observation of J/ψ Pair Production in pp Collisions at \sqrt{s}=7 TeV

Raymond Mountain
Syracuse University

Marina Artuso
Syracuse University

S. Blusk
Syracuse University

Alesandra Borgia
Syracuse University

Follow this and additional works at: https://surface.syr.edu/phy

Part of the Physics Commons

Recommended Citation

Observation of J/ψ pair production in pp collisions at $\sqrt{s} = 7$ TeV

The LHCb Collaboration [1]

Abstract

The production of J/ψ pairs in proton-proton collisions at a centre-of-mass energy of 7 TeV has been observed using an integrated luminosity of 37.5 pb^{-1} collected with the LHCb detector. The production cross-section for pairs with both J/ψ in the rapidity range $2 < y^{\text{J/ψ}} < 4.5$ and transverse momentum $p_{\text{T}}^{\text{J/ψ}} < 10$ GeV/c is

$$\sigma^{\text{J/ψ J/ψ}} = 5.1 \pm 1.0 \pm 1.1 \text{ nb},$$

where the first uncertainty is statistical and the second systematic.

(Submitted to Physics Letters B.)

---

[1]Authors are listed on the following pages.

R. Aaij[23], B. Adeva[36], M. Adinolfi[42], C. Adrover[6], A. Affolder[48], Z. Ajaltouni[5], J. Albrecht[37], F. Alessio[37], M. Alexander[47], G. Alkhazov[29], P. Alvarez Cartelle[36], A.A. Alves Jr[22], S. Amato[2], Y. Amhis[38], J. Anderson[39], R.B. Appleby[50], O. Aquines Gutierrez[10], F. Archilli[18,37], L. Arrabito[53], A. Artamonov [34], M. Artuso[52,37], E. Aslanides[6], G. Auriemma[22,m], S. Bachmann[11], J.J. Back[44], D.S. Bailey[50], V. Balagura[30,37], W. Baldini[16], R.J. Barlow[50], C. Barschel[37], S. Barsuk[7], W. Barter[43], A. Bates[47], C. Bauer[10], Th. Bauer[23], A. Bay[38], I. Bediaga[1], K. Belous[34], I. Belyaev[30,37], E. Ben-Haim[8], M. Benayoun[8], G. Bencivenni[18], S. Benson[46], J. Benton[42], R. Bernet[39], M.-O. Bettler[17], M. van Beuzekom[23], A. Bien[11], S. Bifani[12], A. Bizzeti[17,h], P.M. Bjørnstad[50], T. Blake[49], F. Blanc[38], C. Blanks[49], J. Blouw[11], S. Blusk[52], A. Bobrov[33], V. Bocci[22], A. Bondar[33], N. Bondar[29], W. Bonivento[15], S. Borghi[47], A. Borgia[52], T.J.V. Bowcock[48], C. Bozzi[16], T. Brambach[9], J. van den Brand[24], J. Bressieux[38], D. Brett[50], S. Brisbane[51], M. Britsch[10], T. Britton[52], N.H. Brook[42], H. Brown[48], A. Büchler-Germann[39], I. Burducea[28], A. Bursche[39], J. Buytaert[37], S. Cadeddu[15], J.M. Caicedo Carvajal[37], O. Callot[7], M. Calvi[20,j], M. Calvo Gomez[35,n], A. Camboni[35], P. Campana[18,37], A. Carbone[14], G. Carboni[21,k], R. Cardinale[19,i,37], A. Cardini[15], L. Carson[36], K. Carvalho Akiba[23], G. Casse[48], M. Cattaneo[37], M. Charles[51], Ph. Charpentier[37], N. Chiapolini[39], K. Ciba[37], X. Cid Vidal[36], G. Ciezarek[49], P.E.L. Clarke[46,37], M. Clemencic[37], H.V. Cliff[43], J. Closier[37], C. Coca[28], V. Coco[23], J. Cogan[6], P. Collins[37], F. Constantin[28], G. Conti[38], A. Contu[51], A. Cook[42], M. Coombes[42], G. Corti[37], G.A. Cowan[38], R. Currie[46], B. D'Almagne[7], C. D'Ambrosio[37], P. David[8], I. De Bonis[4], S. De Capua[21,k], M. De Cian[39], F. De Lorenzi[12], J.M. De Miranda[1], L. De Paula[2], P. De Simone[18], D. Decamp[4], M. Deckenhoff[9], H. Degaudenzi[38,37], M. Deissenroth[11], L. Del Buono[8], C. Deplano[15], O. Deschamps[5], F. Dettori[15,d], J. Dickens[43], H. Dijkstra[37], P. Diniz Batista[1], S. Donleavy[48], A. Dosil Suárez[36], D. Dossett[44], A. Dovbnya[40], F. Dupertuis[38], R. Dzhelyadin[34], C. Eames[49], S. Easo[45], U. Egede[49], V. Egorychev[30], S. Eidelman[33], D. van Eijk[23], F. Eisele[11], S. Eisenhardt[46], R. Ekelhof[9], L. Eklund[47], Ch. Elsasser[39], D.G. d'Enterria[35,o], D. Esperante Pereira[36], L. Estève[43], A. Falabella[16,e], E. Fanchini[20,j], C. Färber[11], G. Fardell[46], C. Farinelli[23], S. Farry[12], V. Fave[38], V. Fernandez Albor[36], M. Ferro-Luzzi[37], S. Filippov[32], C. Fitzpatrick[46], M. Fontana[10], F. Fontanelli[19,i], R. Forty[37], M. Frank[37], C. Frei[37], M. Frosini[17,f,37], S. Furcas[20], A. Gallas Torreira[36], D. Galli[14,c], M. Gandelman[2], P. Gandini[51], Y. Gao[3], J-C. Garnier[37], J. Garofoli[52], J. Garra Tico[43], L. Garrido[35], C. Gaspar[37], N. Gauvin[38], M. Gersabeck[37], T. Gershon[44,37], Ph. Ghez[4], V. Gibson[43], V.V. Gligorov[37], C. Göbel[54], D. Golubkov[30], A. Golutvin[49,30,37], A. Gomes[2], H. Gordon[51], M. Grabalosa Gándara[35], R. Graciani Diaz[35], L.A. Granado Cardoso[37], E. Graugés[35], G. Graziani[17], A. Grecu[28], S. Gregson[43], B. Gui[52], E. Gushchin[32], Yu. Guz[34], T. Gys[37], G. Haefeli[38], C. Haen[37], S.C. Haines[43], T. Hampson[42], S. Hansmann-Menzemer[11], R. Harji[49], N. Harnew[51], J. Harrison[50], P.F. Harrison[44], J. He[7], V. Heijne[23], K. Hennessy[48], P. Henrard[5], J.A. Hernando Morata[36], E. van Herwijnen[37], E. Hicks[48], W. Hofmann[10], K. Holubyev[11], P. Hopchev[4], W. Hulsbergen[23], P. Hunt[51], T. Huse[48], R.S. Huston[12], D. Hutchcroft[48], D. Hynds[47], V. Iakovenko[41], P. Ilten[12], J. Imong[42], R. Jacobsson[37], A. Jaeger[11], M. Jahjah Hussein[5], E. Jans[23], F. Jansen[23], P. Jaton[38], B. Jean-Marie[7], F. Jing[3], M. John[51],

iii

D. Johnson[51], C.R. Jones[43], B. Jost[37], S. Kandybei[40], M. Karacson[37], T.M. Karbach[9], J. Keaveney[12], U. Kerzel[37], T. Ketel[24], A. Keune[38], B. Khanji[6], Y.M. Kim[46], M. Knecht[38], S. Koblitz[37], P. Koppenburg[23], A. Kozlinskiy[23], L. Kravchuk[32], K. Kreplin[11], M. Kreps[44], G. Krocker[11], P. Krokovny[11], F. Kruse[9], K. Kruzelecki[37], M. Kucharczyk[20,25,37], S. Kukulak[25], R. Kumar[14,37], T. Kvaratskheliya[30,37], V.N. La Thi[38], D. Lacarrere[37], G. Lafferty[50], A. Lai[15], D. Lambert[46], R.W. Lambert[37], E. Lanciotti[37], G. Lanfranchi[18], C. Langenbruch[11], T. Latham[44], R. Le Gac[6], J. van Leerdam[23], J.-P. Lees[4], R. Lefèvre[5], A. Leflat[31,37], J. Lefrançois[7], O. Leroy[6], T. Lesiak[25], L. Li[3], L. Li Gioi[5], M. Lieng[9], M. Liles[48], R. Lindner[37], C. Linn[11], B. Liu[3], G. Liu[37], J.H. Lopes[2], E. Lopez Asamar[35], N. Lopez-March[38], J. Luisier[38], F. Machefert[7], I.V. Machikhiliyan[4,30], F. Maciuc[10], O. Maev[29,37], J. Magnin[1], S. Malde[51], R.M.D. Mamunur[37], G. Manca[15,d], G. Mancinelli[6], N. Mangiafave[43], U. Marconi[14], R. Märki[38], J. Marks[11], G. Martellotti[22], A. Martens[7], L. Martin[51], A. Martín Sánchez[7], D. Martinez Santos[37], A. Massafferri[1], Z. Mathe[12], C. Matteuzzi[20], M. Matveev[29], E. Maurice[6], B. Maynard[52], A. Mazurov[32,16,37], G. McGregor[50], R. McNulty[12], C. Mclean[14], M. Meissner[11], M. Merk[23], J. Merkel[9], R. Messi[21,k], S. Miglioranzi[37], D.A. Milanes[13,37], M.-N. Minard[4], S. Monteil[5], D. Moran[12], P. Morawski[25], R. Mountain[52], I. Mous[23], F. Muheim[46], K. Müller[39], R. Muresan[28,38], B. Muryn[26], M. Musy[35], J. Mylroie-Smith[48], P. Naik[42], T. Nakada[38], R. Nandakumar[45], J. Nardulli[45], I. Nasteva[1], M. Nedos[9], M. Needham[46], N. Neufeld[37], C. Nguyen-Mau[38,p], M. Nicol[7], S. Nies[9], V. Niess[5], N. Nikitin[31], A. Novoselov[34], A. Oblakowska-Mucha[26], V. Obraztsov[34], S. Oggero[23], S. Ogilvy[47], O. Okhrimenko[41], R. Oldeman[15,d], M. Orlandea[28], J.M. Otalora Goicochea[2], P. Owen[49], B. Pal[52], J. Palacios[39], M. Palutan[18], J. Panman[37], A. Papanestis[45], M. Pappagallo[13,b], C. Parkes[47,37], C.J. Parkinson[49], G. Passaleva[17], G.D. Patel[48], M. Patel[49], S.K. Paterson[49], G.N. Patrick[45], C. Patrignani[19,i], C. Pavel-Nicorescu[28], A. Pazos Alvarez[36], A. Pellegrino[23], G. Penso[22,l], M. Pepe Altarelli[37], S. Perazzini[14,c], D.L. Perego[20,j], E. Perez Trigo[36], A. Pérez-Calero Yzquierdo[35], P. Perret[5], M. Perrin-Terrin[6], G. Pessina[20], A. Petrella[16,37], A. Petrolini[19,i], B. Pie Valls[35], B. Pietrzyk[4], T. Pilar[44], D. Pinci[22], R. Plackett[47], S. Playfer[46], M. Plo Casasus[36], G. Polok[25], A. Poluektov[44,33], E. Polycarpo[2], D. Popov[10], B. Popovici[28], C. Potterat[35], A. Powell[51], T. du Pree[23], J. Prisciandaro[38], V. Pugatch[41], A. Puig Navarro[35], W. Qian[52], J.H. Rademacker[42], B. Rakotomiaramanana[38], M.S. Rangel[2], I. Raniuk[40], G. Raven[24], S. Redford[51], M.M. Reid[44], A.C. dos Reis[1], S. Ricciardi[45], K. Rinnert[48], D.A. Roa Romero[5], P. Robbe[7], E. Rodrigues[47], F. Rodrigues[2], P. Rodriguez Perez[36], G.J. Rogers[43], S. Roiser[37], V. Romanovsky[34], J. Rouvinet[38], T. Ruf[37], H. Ruiz[35], G. Sabatino[21,k], J.J. Saborido Silva[36], N. Sagidova[29], P. Sail[47], B. Saitta[15,d], C. Salzmann[39], M. Sannino[19,i], R. Santacesaria[22], R. Santinelli[37], E. Santovetti[21,k], M. Sapunov[6], A. Sarti[18,l], C. Satriano[22,m], A. Satta[21], M. Savrie[16,e], D. Savrina[30], P. Schaack[49], M. Schiller[11], S. Schleich[9], M. Schmelling[10], B. Schmidt[37], O. Schneider[38], A. Schopper[37], M.-H. Schune[7], R. Schwemmer[37], A. Sciubba[18,l], M. Seco[36], A. Semennikov[30], K. Senderowska[26], I. Sepp[49], N. Serra[39], J. Serrano[6], P. Seyfert[11], B. Shao[3], M. Shapkin[34], I. Shapoval[40,37], P. Shatalov[30], Y. Shcheglov[29], T. Shears[48], L. Shekhtman[33], O. Shevchenko[40], V. Shevchenko[30], A. Shires[49], R. Silva Coutinho[54], H.P. Skottowe[43], T. Skwarnicki[52], A.C. Smith[37], N.A. Smith[48], K. Sobczak[5],

F.J.P. Soler[47], A. Solomin[42], F. Soomro[49], B. Souza De Paula[2], B. Spaan[9], A. Sparkes[46], P. Spradlin[47], F. Stagni[37], S. Stahl[11], O. Steinkamp[39], S. Stoica[28], S. Stone[52,37], B. Storaci[23], M. Straticiuc[28], U. Straumann[39], N. Styles[46], V.K. Subbiah[37], S. Swientek[9], M. Szczekowski[27], P. Szczypka[38], T. Szumlak[26], S. T'Jampens[4], E. Teodorescu[28], F. Teubert[37], C. Thomas[51,45], E. Thomas[37], J. van Tilburg[11], V. Tisserand[4], M. Tobin[39], S. Topp-Joergensen[51], M.T. Tran[38], A. Tsaregorodtsev[6], N. Tuning[23], A. Ukleja[27], P. Urquijo[52], U. Uwer[11], V. Vagnoni[14], G. Valenti[14], R. Vazquez Gomez[35], P. Vazquez Regueiro[36], S. Vecchi[16], J.J. Velthuis[42], M. Veltri[17,g], K. Vervink[37], B. Viaud[7], I. Videau[7], X. Vilasis-Cardona[35,n], J. Visniakov[36], A. Vollhardt[39], D. Voong[42], A. Vorobyev[29], H. Voss[10], K. Wacker[9], S. Wandernoth[11], J. Wang[52], D.R. Ward[43], A.D. Webber[50], D. Websdale[49], M. Whitehead[44], D. Wiedner[11], L. Wiggers[23], G. Wilkinson[51], M.P. Williams[44,45], M. Williams[49], F.F. Wilson[45], J. Wishahi[9], M. Witek[25,37], W. Witzeling[37], S.A. Wotton[43], K. Wyllie[37], Y. Xie[46], F. Xing[51], Z. Yang[3], R. Young[46], O. Yushchenko[34], M. Zavertyaev[10,a], L. Zhang[52], W.C. Zhang[12], Y. Zhang[3], A. Zhelezov[11], L. Zhong[3], E. Zverev[31], A. Zvyagin [37].

[1]*Centro Brasileiro de Pesquisas Físicas (CBPF), Rio de Janeiro, Brazil*
[2]*Universidade Federal do Rio de Janeiro (UFRJ), Rio de Janeiro, Brazil*
[3]*Center for High Energy Physics, Tsinghua University, Beijing, China*
[4]*LAPP, Université de Savoie, CNRS/IN2P3, Annecy-Le-Vieux, France*
[5]*Clermont Université, Université Blaise Pascal, CNRS/IN2P3, LPC, Clermont-Ferrand, France*
[6]*CPPM, Aix-Marseille Université, CNRS/IN2P3, Marseille, France*
[7]*LAL, Université Paris-Sud, CNRS/IN2P3, Orsay, France*
[8]*LPNHE, Université Pierre et Marie Curie, Université Paris Diderot, CNRS/IN2P3, Paris, France*
[9]*Fakultät Physik, Technische Universität Dortmund, Dortmund, Germany*
[10]*Max-Planck-Institut für Kernphysik (MPIK), Heidelberg, Germany*
[11]*Physikalisches Institut, Ruprecht-Karls-Universität Heidelberg, Heidelberg, Germany*
[12]*School of Physics, University College Dublin, Dublin, Ireland*
[13]*Sezione INFN di Bari, Bari, Italy*
[14]*Sezione INFN di Bologna, Bologna, Italy*
[15]*Sezione INFN di Cagliari, Cagliari, Italy*
[16]*Sezione INFN di Ferrara, Ferrara, Italy*
[17]*Sezione INFN di Firenze, Firenze, Italy*
[18]*Laboratori Nazionali dell'INFN di Frascati, Frascati, Italy*
[19]*Sezione INFN di Genova, Genova, Italy*
[20]*Sezione INFN di Milano Bicocca, Milano, Italy*
[21]*Sezione INFN di Roma Tor Vergata, Roma, Italy*
[22]*Sezione INFN di Roma La Sapienza, Roma, Italy*
[23]*Nikhef National Institute for Subatomic Physics, Amsterdam, Netherlands*
[24]*Nikhef National Institute for Subatomic Physics and Vrije Universiteit, Amsterdam, Netherlands*
[25]*Henryk Niewodniczanski Institute of Nuclear Physics Polish Academy of Sciences, Cracow, Poland*
[26]*Faculty of Physics & Applied Computer Science, Cracow, Poland*
[27]*Soltan Institute for Nuclear Studies, Warsaw, Poland*
[28]*Horia Hulubei National Institute of Physics and Nuclear Engineering, Bucharest-Magurele, Romania*
[29]*Petersburg Nuclear Physics Institute (PNPI), Gatchina, Russia*
[30]*Institute of Theoretical and Experimental Physics (ITEP), Moscow, Russia*
[31]*Institute of Nuclear Physics, Moscow State University (SINP MSU), Moscow, Russia*
[32]*Institute for Nuclear Research of the Russian Academy of Sciences (INR RAN), Moscow, Russia*
[33]*Budker Institute of Nuclear Physics (SB RAS) and Novosibirsk State University, Novosibirsk, Russia*

[34] *Institute for High Energy Physics (IHEP), Protvino, Russia*

[35] *Universitat de Barcelona, Barcelona, Spain*

[36] *Universidad de Santiago de Compostela, Santiago de Compostela, Spain*

[37] *European Organization for Nuclear Research (CERN), Geneva, Switzerland*

[38] *Ecole Polytechnique Fédérale de Lausanne (EPFL), Lausanne, Switzerland*

[39] *Physik-Institut, Universität Zürich, Zürich, Switzerland*

[40] *NSC Kharkiv Institute of Physics and Technology (NSC KIPT), Kharkiv, Ukraine*

[41] *Institute for Nuclear Research of the National Academy of Sciences (KINR), Kyiv, Ukraine*

[42] *H.H. Wills Physics Laboratory, University of Bristol, Bristol, United Kingdom*

[43] *Cavendish Laboratory, University of Cambridge, Cambridge, United Kingdom*

[44] *Department of Physics, University of Warwick, Coventry, United Kingdom*

[45] *STFC Rutherford Appleton Laboratory, Didcot, United Kingdom*

[46] *School of Physics and Astronomy, University of Edinburgh, Edinburgh, United Kingdom*

[47] *School of Physics and Astronomy, University of Glasgow, Glasgow, United Kingdom*

[48] *Oliver Lodge Laboratory, University of Liverpool, Liverpool, United Kingdom*

[49] *Imperial College London, London, United Kingdom*

[50] *School of Physics and Astronomy, University of Manchester, Manchester, United Kingdom*

[51] *Department of Physics, University of Oxford, Oxford, United Kingdom*

[52] *Syracuse University, Syracuse, NY, United States*

[53] *CC-IN2P3, CNRS/IN2P3, Lyon-Villeurbanne, France, associated member*

[54] *Pontifícia Universidade Católica do Rio de Janeiro (PUC-Rio), Rio de Janeiro, Brazil, associated to [2]*

[a] *P.N. Lebedev Physical Institute, Russian Academy of Science (LPI RAS), Moscow, Russia*

[b] *Università di Bari, Bari, Italy*

[c] *Università di Bologna, Bologna, Italy*

[d] *Università di Cagliari, Cagliari, Italy*

[e] *Università di Ferrara, Ferrara, Italy*

[f] *Università di Firenze, Firenze, Italy*

[g] *Università di Urbino, Urbino, Italy*

[h] *Università di Modena e Reggio Emilia, Modena, Italy*

[i] *Università di Genova, Genova, Italy*

[j] *Università di Milano Bicocca, Milano, Italy*

[k] *Università di Roma Tor Vergata, Roma, Italy*

[l] *Università di Roma La Sapienza, Roma, Italy*

[m] *Università della Basilicata, Potenza, Italy*

[n] *LIFAELS, La Salle, Universitat Ramon Llull, Barcelona, Spain*

[o] *Institució Catalana de Recerca i Estudis Avançats (ICREA), Barcelona, Spain*

[p] *Hanoi University of Science, Hanoi, Viet Nam*

1 Introduction

The mechanism of heavy quarkonium production is a long-standing problem in QCD. An effective field theory, non-relativistic QCD (NRQCD), provides the foundation for much of the current theoretical work. According to NRQCD, the production of heavy quarkonium factorizes into two steps: a heavy quark-antiquark pair is first created perturbatively at short distances and subsequently evolves non-perturbatively into quarkonium at long distances. The NRQCD calculations depend on the colour-singlet (CS) and colour-octet (CO) matrix elements, which account for the probability of a heavy quark-antiquark pair in a particular colour state to evolve into heavy quarkonium.

The CS model [1, 2], which provides a leading-order (LO) description of quarkonia production, was first used to describe experimental data. However, it underestimates the observed cross-section for single J/ψ production at high p_{T} at the Tevatron [3]. To resolve this discrepancy the CO mechanism was introduced [4]. The corresponding matrix elements were determined from the large-p_{T} data as the CO cross-section falls more slowly than the CS one. However, recent calculations [5, 6, 7, 8] close the gap between the CS predictions and the experimental data [9] reducing the need for large CO contributions. Thus, further experimental tests are needed. Pair production of quarkonium can cast light on this problem as this process depends heavily on the production mechanism. For both the CS and CO models, contributions from double parton scattering [10, 11, 12] could potentially be significant.

The only observation of pair charmonia production in hadronic collisions to date was by the NA3 collaboration, who found evidence for J/ψ pair production in multi-muon events in pion-platinum interactions at pion momenta of 150 and 280 GeV/c [13] and in proton-platinum interactions at a proton momentum of 400 GeV/c [14]. The cross-section ratio $\sigma^{\mathrm{J}/\psi\,\mathrm{J}/\psi}/\sigma^{\mathrm{J}/\psi}$ was measured to be $(3 \pm 1) \times 10^{-4}$ for pion-induced production, where $\sigma^{\mathrm{J}/\psi}$ is the inclusive J/ψ production cross-section. At NA3 energies the main contribution to the J/ψ pair cross-section arises from the quark-antiquark annihilation channel [15]. This is not the case for proton-proton collisions at the LHC, where the gluon-gluon fusion process dominates [16, 17].

Theoretical calculations based on the LO production of CS-states predict that the total cross-section for J/ψ-pair production in proton-proton interactions at $\sqrt{s} = 7$ TeV is equal to 24 nb [18, 19]. These calculations take into account both direct production and feeddown from $\psi(2S)$ decays but do not include the possible contribution from double parton scattering. In the rapidity interval $2.0 < y^{\mathrm{J}/\psi} < 4.5$, relevant to the LHCb experiment, the expected value is 4 nb with uncertainty of around 30%. At small invariant masses of the J/ψ pair a tetraquark state, built from four c-quarks, may exist [19] and would be visible as a narrow resonance in the mass spectrum.

2 The LHCb detector and dataset

The LHCb detector is a forward spectrometer [20] providing charged particle reconstruction in the pseudorapidity range $1.9 < \eta < 4.9$. The detector elements are placed along

the beam line of the LHC starting with the Vertex Locator, a silicon strip device that surrounds the proton-proton interaction region. This reconstructs precisely the locations of interaction vertices, the locations of decays of long-lived hadrons and contributes to the measurement of track momenta. Other detectors used to measure track momenta comprise a large area silicon strip detector located upstream of a dipole magnet with bending power around 4 Tm and a combination of silicon strip detectors and straw drift-tubes placed downstream. Two ring imaging Cherenkov detectors are used to identify charged hadrons. Further downstream, an electromagnetic calorimeter is used for photon and electron identification, followed by a hadron calorimeter and a muon system consisting of alternating layers of iron and chambers (MWPC and triple-GEM) that distinguishes muons from hadrons. The calorimeters and muon system provide the capability of first-level hardware triggering.

The LHCb trigger system consists of three levels. The first level (L0) is designed to reduce the LHC bunch crossing rate of 40 MHz to a maximum of 1 MHz, at which the complete detector is read out. This is the input to the first stage of the software trigger, which performs a partial event reconstruction to confirm or discard the L0 trigger decision. The second stage of the software trigger performs a full event reconstruction to further discriminate signal events from other pp collisions. To avoid that a few events with high occupancy dominate the CPU time, a set of global event cuts is applied on the hit multiplicities of each sub-detector used by the pattern recognition algorithms. These cuts were chosen to reject high-multiplicity events with a large number of pp interactions with minimal loss of luminosity.

The data used for this analysis comprise an integrated luminosity of $37.5 \, \text{pb}^{-1}$ of pp collisions at a centre-of-mass energy of 7 TeV collected by the LHCb experiment between July and November 2010. During this period all detector components were fully operational and in a stable condition. The mean number of visible proton-proton collisions per bunch crossing was up to 2.5.

The simulation samples used are based on the PYTHIA 6.4 generator [21] configured with the parameters detailed in Ref. [22]. The EVTGEN [23] and GEANT4 [24] packages are used to generate hadron decays and simulate interactions in the detector, respectively. Prompt charmonium production is generated in PYTHIA according to the leading order CS and CO mechanisms.

3 Event selection and signal yield

In this analysis the J/ψ is reconstructed through its decay into a pair of muons. The selection starts by forming $\text{J}/\psi \to \mu^+\mu^-$ candidates from pairs of oppositely-charged particles identified as muons that each have a transverse momentum greater than 650 MeV/c and that originate from a common vertex. Track quality is ensured by requiring that the $\chi^2_{\text{tr}}/\text{ndf}$ provided by the track fit is less than five. Well identified muons are selected by requiring that the difference in logarithms of the global likelihood of the muon hypothesis, provided by the particle identification detectors, with respect to the hadron hypothesis,

2

$\Delta \ln \mathcal{L}^{\mu-\mathrm{h}}$, be greater than zero. To suppress the contribution from duplicate particles created by the reconstruction, if two particles have a symmetrized Kullback-Leibler divergence [25] less than 5000, only the particle with the best track fit is considered.

Selected $\mu^+\mu^-$ candidates with an invariant mass in the range $3.0 < m_{\mu^+\mu^-} < 3.2 \,\mathrm{GeV}/c^2$ are paired to form $(\mu^+\mu^-)_1(\mu^+\mu^-)_2$ combinations. A fit of the four-muon candidate is performed [26] that requires the four tracks to be consistent with originating from a common vertex and that this vertex is compatible with one of the reconstructed pp collision vertices. To reject background where two J/ψ candidates originates from different pp collisions, the reduced χ^2 of this fit, $\chi^2_{\mathrm{DTF}}/\mathrm{ndf}$, is required to be less than five.

The number of events with two J/ψ mesons is extracted from the single J/ψ mass spectra. The invariant mass distributions of the first dimuon pair are obtained in bins of the invariant mass of the second pair[2]. The single J/ψ mass spectrum is modelled empirically using the simulation. This exhibits non-Gaussian tails on either side of the peak. The tail on the left-hand side is dominated by radiative effects in J/ψ decay, while the right-hand side tail is due to non-Gaussian effects in the recontruction. The shape of distribution is described by a function that is similar to Crystal Ball function [27, 28], but with the power-law tails on both sides of the core Gaussian component. The position of the J/ψ peak, the effective mass resolution and the tail parameters of this double-sided Crystal Ball function are fixed to the values determined from an analysis of the signal shape in the inclusive J/ψ sample. Combinatorial background is modelled using an exponential function. The yield of $\mathrm{J/}\psi \to (\mu^+\mu^-)_1$ in bins of the $(\mu^+\mu^-)_2$ invariant mass is shown in Fig. 1a together with the result of a fit according to the model described above. The yield of events with double J/ψ production given by the fit is $N^{\mathrm{J/}\psi\,\mathrm{J/}\psi} = 141 \pm 19$, where the statistical significance of this signal exceeds 6σ. A fit with position and resolution of the signal peak left free was also performed and gave consistent results.

Studies of single J/ψ production indicate that the detector acceptance and efficiency is high for the fiducial range $2 < y^{\mathrm{J/}\psi} < 4.5$ and $p_{\mathrm{T}}^{\mathrm{J/}\psi} < 10 \,\mathrm{GeV}/c$. The raw yield of events with both J/ψ mesons within this range is 139 ± 18. The yield of events with both J/ψ mesons in the fiducial range and explicitly triggered by one of the J/ψ candidates is found to be 116 ± 16.

The contribution to the yield from the pileup of two interactions each producing a single J/ψ meson is estimated using simulation together with the measured J/ψ production cross-section [29]. This study shows that for the 2010 data-taking conditions the background from this source is expected to be less than 1.5 events and hence can be neglected.

4 Efficiency evaluation

The per-event efficiency for a J/ψ-pair event, $\varepsilon_{\mathrm{J/}\psi\,\mathrm{J/}\psi}^{\mathrm{tot}}$, is decomposed into three factors,

$$\varepsilon_{\mathrm{J/}\psi\,\mathrm{J/}\psi}^{\mathrm{tot}} = \varepsilon_{\mathrm{J/}\psi\,\mathrm{J/}\psi}^{\mathrm{reco}} \times \varepsilon_{\mathrm{J/}\psi\,\mathrm{J/}\psi}^{\mu\mathrm{ID}} \times \varepsilon_{\mathrm{J/}\psi\,\mathrm{J/}\psi}^{\mathrm{trg}}, \tag{1}$$

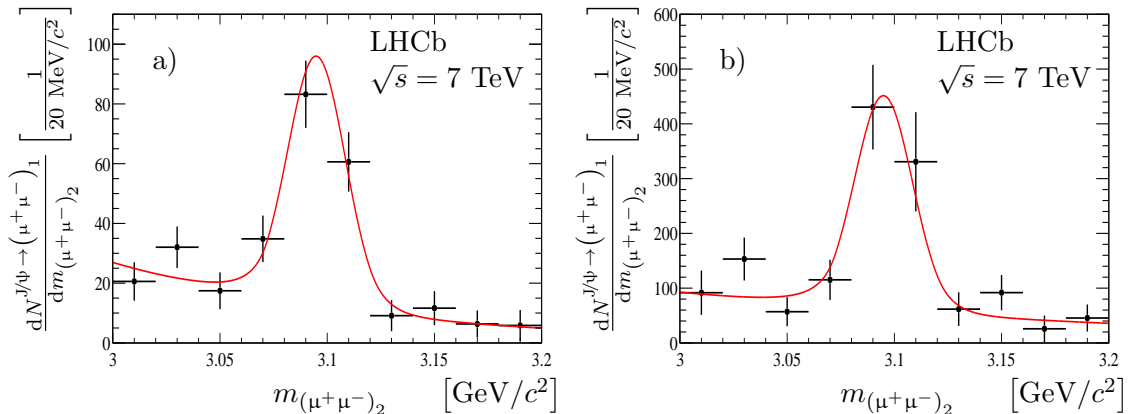[2] The $\mu^+\mu^-$ pair with lower transverse momentum is chosen to be the first pair.

Figure 1: The fitted yields of $J/\psi \to (\mu^+\mu^-)_1$ in bins of $(\mu^+\mu^-)_2$ invariant mass: (a) the raw signal yield observed in the data; (b) the efficiency corrected yield (Sect. 6). The result of a fit with a double-sided Crystal Ball function for the signal and an exponential background is superimposed.

where $\varepsilon^{\rm reco}_{J/\psi\,J/\psi}$ is the efficiency for acceptance, reconstruction and selection, $\varepsilon^{\mu\rm ID}_{J/\psi\,J/\psi}$ is the efficiency for muon identification and $\varepsilon^{\rm trg}_{J/\psi\,J/\psi}$ is the trigger efficiency for reconstructed and selected events.

The efficiency for the acceptance, reconstruction and selection for the two J/ψ mesons is factorized into the product of efficiencies for the first and second J/ψ,

$$\varepsilon^{\rm reco}_{J/\psi\,J/\psi} = \varepsilon^{\rm reco}_{J/\psi}\left(p_{\rm T}^{J/\psi_1}, y^{J/\psi_1}, |\cos\vartheta^*_{J/\psi_1}|\right) \times \varepsilon^{\rm reco}_{J/\psi}\left(p_{\rm T}^{J/\psi_2}, y^{J/\psi_2}, |\cos\vartheta^*_{J/\psi_2}|\right). \qquad (2)$$

The single J/ψ efficiency $\varepsilon^{\rm reco}_{J/\psi}$ is a function of the transverse momentum $p_{\rm T}$, rapidity y and $|\cos\vartheta^*|$, where ϑ^* is the angle between the μ^+ momentum in the J/ψ centre-of-mass frame and the J/ψ flight direction in the laboratory frame. It is evaluated using simulation. The validity of the factorization hypothesis of Eq. (2) is checked with simulation and based on these studies a correction factor of 0.975 is applied to $\varepsilon^{\rm reco}_{J/\psi\,J/\psi}$. For the simulated data of single prompt J/ψ production the cut on the muon likelihood is not applied and that on $\chi^2_{\rm DTF}(J/\psi\,J/\psi)/{\rm ndf}$ is replaced with a similar cut on the single J/ψ, $\chi^2_{\rm DTF}(J/\psi)/{\rm ndf} < 5$. The efficiency of the cut on $\chi^2_{\rm DTF}/{\rm ndf}$ is estimated from the data and compared to the simulation. Based on these studies a correction factor of 1.026 is applied to $\varepsilon^{\rm reco}_{J/\psi\,J/\psi}$, and a systematic uncertainty of 3% is assigned. The efficiency $\varepsilon^{\rm reco}_{J/\psi}$ is also corrected by a factor 1.024 ± 0.011 [29], that accounts for the ratio of the reconstruction efficiency of the muon detector observed in the data compared to the simulation.

The muon identification efficiency is extracted from the analysis of the inclusive J/ψ sample. Two efficiencies are evaluated: the single muon identification efficiency $\varepsilon^{\mu\rm ID}_\mu$ and the J/ψ efficiency $\varepsilon^{\mu\rm ID}_{J/\psi}$. Both are measured as a function of the value of the cut made on $\Delta\ln\mathcal{L}^{\mu-h}$. The squared efficiency $(\varepsilon^{\mu\rm ID}_{1\mu})^2$ and $\varepsilon^{\mu\rm ID}_{J/\psi}$ are found to be equal to better than one per mille. The value of $\varepsilon^{\mu\rm ID}_{J/\psi\,J/\psi} = (\varepsilon^{\mu\rm ID}_{J/\psi})^2 = (91.0 \pm 0.1)\%$ has been used

as a global factor for the evaluation of the total efficiency using Eq. (1). As a cross-check, the efficiency of the muon identification for J/ψ pairs has been estimated from the signal itself. Though statistically limited, the value is consistent with that given above.

The trigger efficiency is calculated to be

$$\varepsilon_{\text{J/}\psi\,\text{J/}\psi}^{\text{trg}} = 1 - \left(1 - \varepsilon_{\text{J/}\psi}^{\text{trg}}\left(p_{\text{T}}^{\text{J/}\psi_1}, y^{\text{J/}\psi_1}\right)\right) \times \left(1 - \varepsilon_{\text{J/}\psi}^{\text{trg}}\left(p_{\text{T}}^{\text{J/}\psi_2}, y^{\text{J/}\psi_2}\right)\right). \tag{3}$$

The trigger efficiency for a single J/ψ, $\varepsilon_{\text{J/}\psi}^{\text{trg}}$, is determined directly on data from the inclusive prompt J/ψ sample as a function of the transverse momentum p_{T} and rapidity y using a method that exploits the fact that J/ψ events can be triggered either by the J/ψ daughters or by the rest of the event [30]. The overlap between the two cases allows the trigger efficiency to be calculated from the data. The effect of the global event cuts applied in the trigger has been studied in detail for inclusive J/ψ events in Ref. [29]. Since the subdetector hit multiplicity observed in single and double J/ψ events is similar, the efficiency of the global event cuts, $(93 \pm 2)\%$, is taken from that study and applied to $\varepsilon_{\text{J/}\psi\,\text{J/}\psi}^{\text{trg}}$.

5 Systematic uncertainties

Systematic uncertainties affecting the cross-section measurement have been evaluated properly taking correlations into account where appropriate. The dominant source of systematic uncertainty is due to the knowledge of the track-finding efficiency. An uncertainty of 4% per track is assigned based on studies comparing the reconstruction efficiency in data and simulation using a tag and probe approach [30].

The second major source of uncertainty is due to the evaluation of the trigger efficiency. The method discussed in Sect. 4 has been cross-checked in several ways, in particular, by using events triggered by the first or second J/ψ only. The observed differences lead to the assignment of an 8% systematic uncertainty.

A further source of uncertainty is the determination of the per-event efficiency defined by Eq. (1). This is estimated to be 3% by varying the uncertainties of the various factors entering into Eq. (1).

The unknown polarization of J/ψ mesons affects the acceptance, reconstruction and selection efficiency $\varepsilon_{\text{J/}\psi}^{\text{reco}}$ [29]. In this analysis the effect is reduced by explicitly taking into account the dependence of the acceptance on $\varepsilon_{\text{J/}\psi}^{\text{reco}}$ on $|\cos\vartheta^*|$ in the efficiency determination (Eq. 2). The remaining dependence results in a systematic uncertainity of 5% per J/ψ.

Additional systematic uncertainties arise due to the difference observed between the data and simulation for the behaviour of the cut on χ_{DTF}^2 (3%), the global event cuts (2%), and uncertainty of 1.1% per J/ψ associated with the efficiency for muon identification, as discussed in Sect. 4. The systematic uncertainties associated with the other selection criteria and the J/ψ lineshape parametrization are negligible.

The luminosity was measured at specific periods during the data taking using both van der Meer scans [31] and a beam-gas imaging method [32]. The instantaneous luminosity determinaton is then based on a continuous recording of the multiplicity of tracks

Table 1: Relative systematic uncertainties on the cross-section measurement, the total uncertainty is calculated as the quadratic sum of the individual components.

Source	Systematic uncertainty [%]
Track finding efficiency	4×4
Trigger efficiency	8
Per-event efficiency	3
J/ψ polarization	2×5
Data/simulation difference for χ^2_{DTF}	3
Global event cuts	2
Muon identification	2×1.1
Luminosity	3.5
J/$\psi \to \mu^+\mu^-$ branching ratio	2×1
Total	21

reconstructed in Vertex Locator, which has been normalized to the absolute luminosity scale. Consistent results are found for the absolute luminosity scale with a precision of 3.5%, dominated by the beam current uncertainty [33].

The relative systematic uncertainties are summarized in Table 1, where the total uncertainty is defined as the quadratic sum of the individual components.

6 Cross-section determination

The efficiency-corrected yield for events with both J/ψ in the fiducial region is extracted using the procedure discussed in Sect. 3. To account for the efficiency a weight ω, defined as

$$\omega^{-1} = \varepsilon^{\mathrm{tot}}_{\mathrm{J}/\psi\,\mathrm{J}/\psi} \tag{4}$$

where $\varepsilon^{\mathrm{tot}}_{\mathrm{J}/\psi\,\mathrm{J}/\psi}$ is the total efficiency defined in Eq. (1), is applied to each candidate in the sample.

The corrected yield of J/$\psi \to (\mu^+\mu^-)_1$ in bins of $(\mu^+\mu^-)_2$ invariant mass is shown in Fig. 1b. As previously described, to extract the yield a fit with a double-sided Crystal Ball function for the signal, together with an exponential function for the background component, is performed. Again, the position of the J/ψ peak and the effective mass resolution are fixed to the values found in the inclusive J/ψ sample. The event yield after the efficiency correction is

$$N^{\mathrm{corr}}_{\mathrm{J}/\psi\,\mathrm{J}/\psi} = 672 \pm 129. \tag{5}$$

The cross-section for double J/ψ production in the fiducial range $2 < y^{\mathrm{J}/\psi} < 4.5$ and $p_{\mathrm{T}}^{\mathrm{J}/\psi} < 10$ GeV/c is computed as

$$\sigma^{\mathrm{J}/\psi\,\mathrm{J}/\psi} = \frac{N^{\mathrm{corr}}_{\mathrm{J}/\psi\,\mathrm{J}/\psi}}{\mathcal{L} \times \mathcal{B}^2_{\mu^+\mu^-}},$$

where $\mathcal{L} = 37.5 \pm 1.3$ pb^{-1} is the integrated luminosity and $\mathcal{B}_{\mu^+\mu^-} = (5.93 \pm 0.06)\%$ [34] is the J/$\psi \to \mu^+\mu^-$ branching ratio. The result is

$$\sigma^{\text{J/}\psi\,\text{J/}\psi} = 5.1 \pm 1.0 \pm 1.1 \text{ nb},$$

where the first uncertainty is statistical and the second systematic.

The differential production cross-section of J/ψ pairs as a function of the invariant mass of the J/ψ J/ψ system is shown in Fig. 2. The bulk of the distribution is concentrated in the low invariant mass region. A theoretical prediction for the shape of this distribution taking into account both direct production and feeddown from $\psi(2S)$ decays [19] is overlaid. Within the available statistics the agreement between the data and the prediction is reasonable.
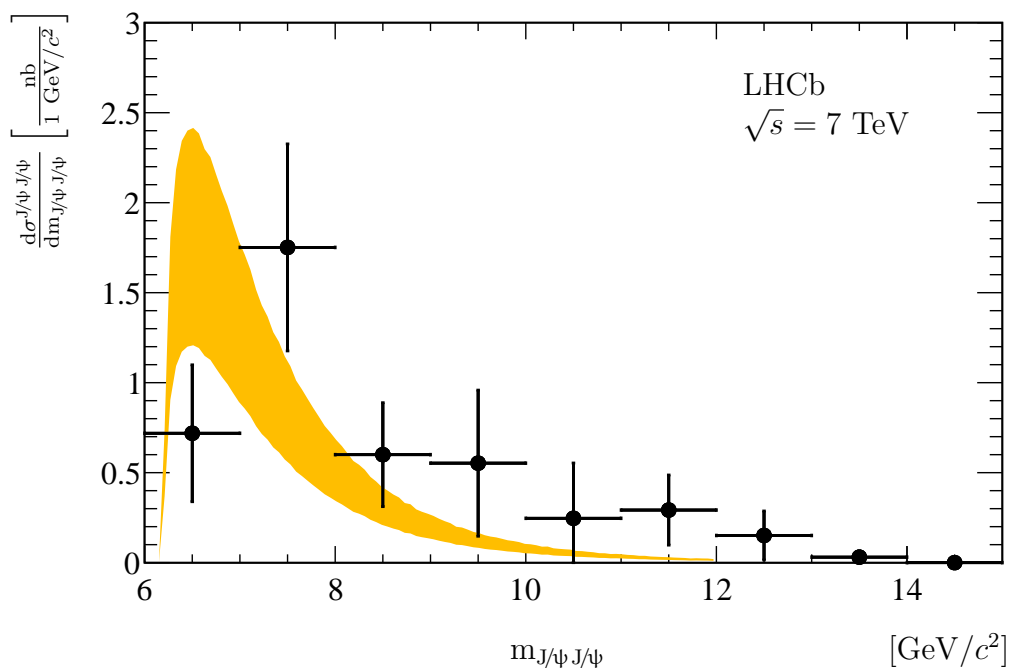

Figure 2: Differential production cross-section for J/ψ pairs as a function of the invariant mass of the J/ψ J/ψ system. The points correspond to the data. Only the statistical uncertainties are included in the error bars. The shaded area corresponds to prediction by the model described in Ref. [19].

7 Conclusions

The production of J/ψ pairs in proton-proton collisions at a centre-of-mass energy of 7 TeV has been observed with a statistical significance in excess of 6σ. The data are consistent with the predictions given in Refs. [18, 19]. The higher statistics that will be collected during the 2011 data-taking period will allow the kinematic properties of these events to be studied and different production models to be probed.

Acknowledgments

References

[1] V.G. Kartvelishvili, A.K. Likhoded and S.R. Slabospitsky, "D meson and ψ meson production in hadronic interactions", Sov. J. Nucl. Phys. **28**, 678 (1978) [Yad. Fiz. **28**, 1315 (1978)].

[2] R. Baier and R. Ruckl, "Hadronic production of J/ψ and Υ: transverse momentum distributions", Phys. Lett. B **102**, 364 (1981).

[3] F. Abe *et al.*, "Inclusive J/ψ, $\psi(2S)$ and b-quark production in $\bar{p}$p-collisions at $\sqrt{s} = 1.8$ TeV", Phys. Rev. Lett. **69**, 3704 (1992).

[4] E. Braaten and S. Fleming, "Color octet fragmentation and the ψ'-surplus at the Tevatron", Phys. Rev. Lett. **74**, 3327 (1995).

[5] J.M. Campbell, F. Maltoni and F. Tramontano, "QCD corrections to J/ψ and Υ production at hadron colliders", Phys. Rev. Lett. **98**, 252002 (2007).

[6] B. Gong and J.X. Wang, "Next-to-leading-order QCD corrections to J/ψ polarization at Tevatron and Large-Hadron-Collider energies", Phys. Rev. Lett. **100**, 232001 (2008).

[7] P. Artoisenet, J.M. Campbell, J.-P. Lansberg, F. Maltoni and F. Tramontano, "Υ production at Fermilab Tevaton and LHC energies", Phys. Rev. Lett. **101**, 152001 (2008).

[8] J.-P. Lansberg, "On the mechanisms of heavy-quarkonium hadroproduction", Eur. Phy. J. **C61**, 693 (2009).

[9] N. Brambilla *et al.*, "Heavy quarkonium: progress, puzzles, and opportunities", Eur. Phy. J. **C71**, 1534 (2011).

[10] C.H. Kom, A. Kulesza and W.J. Stirling, "Pair production of J/ψ as a probe of double parton scattering at LHCb", arXiv:1105.4186 [hep-ph].

[11] S.P. Baranov, A.M. Snigirev and N.P. Zotov, "Double heavy meson production through double parton scattering in hadronic collisions", arXiv:1105.6276 [hep-ph].

[12] A. Novoselov, "Double parton scattering as a source of quarkonia pairs in LHCb", arXiv:1106.2184 [hep-ph].

[13] J. Badier *et al.*, "Evidence for ψψ production in π^- interactions at 150 GeV/c and 280 GeV/c", Phys. Lett. B **114**, 457 (1982).

[14] J. Badier *et al.*, "ψψ production and limits on beauty meson production from 400 GeV/c protons", Phys. Lett. B **158**, 85 (1985).

[15] V.G. Kartvelishvili and S.M. Esakiya, "On hadron induced production of J/ψ meson pairs", Yad. Fiz. **38**, 722 (1983).

[16] B. Humpert and P. Mery, " ψψ production at collider energies", Z. Phys. C **20**, 83 (1983).

[17] V.V. Kiselev, A.K. Likhoded, S.R. Slabospitsky and A.V. Tkabladze, "Hadronic pair production of ψ particles with large $M(ψψ)$," Sov. J. Nucl. Phys. **49**, 1041 (1989) [Yad. Fiz. **49**, 1681 (1989)].

[18] C.F. Qiao, L.P. Sun and P. Sun, "Testing charmonium production mechanism via polarized J/ψ-pair production at the LHC", J. Phys. G **37**, 075019 (2010).

[19] A.V. Berezhnoy, A.K. Likhoded, A.V. Luchinsky and A.A. Novoselov, "Double J/ψ meson production at LHC and 4c-tetraquark state", arXiv:1101.5881 [hep-ph].

[20] A.A. Alves *et al.*, "The LHCb detector at LHC", JINST **3**, S08005 (2008).

[21] T. Sjöstrand, S. Mrenna and P. Z. Skands, "PYTHIA 6.4 physics and manual", JHEP **05**, 026 (2006), version 6.422, arXiv:hep-ph/0603175.

[22] I. Belyaev *et al.*, "Handling of the generation of primary events in GAUSS, the LHCb simulation framework", Nuclear Sceince Symposium Conference Record (NSS/MIC), IEEE, 1155 (2010).

[23] D. Lange, "The EVTGEN particle decay simulation package", Nucl. Instrum. Meth. A **462**, 152 (2001).

[24] S. Agostinelli *et al.*, "GEANT4: a simulation toolkit", Nucl. Instrum. Meth. A **506**, 250 (2003).

[25] S. Kullback and R.A. Leibler, "On information and sufficiency", Annals of Mathematical Statistics **22**, 79 (1951);
S. Kullback, "Letter to editor: the Kullback-Leibler distance", The American Statistician **41**, 340 (1987).

[26] W.D. Hulsbergen, "Decay chain fitting with a Kalman filter", Nucl. Instrum. Meth. A **552**, 566 (2005).

[27] J.E. Gaiser, "Charmonium spectroscopy from radiative decays of the J/ψ and ψ'", Ph.D. Thesis, SLAC-R-255 (1982).

[28] T. Skwarnicki, "A study of the radiative cascade transitions between the Υ' and Υ resonances", Ph.D. Thesis, DESY-F31-86-02 (1986).

[29] R. Aaij *et al.*, "Measurement of J/ψ production in pp collisions at $\sqrt{s} = 7$ TeV", Eur. Phy. J. C **71**, 1645 (2011).

[30] R. Aaij *et al.*, "Prompt K_S^0 production in pp collisions at $\sqrt{s} = 0.9$ TeV", Phys. Lett. B **693**, 69 (2010).

[31] S. van der Meer, "Calibration of the effective beam height in the ISR", ISR-PO/68-31 (1968).

[32] M. Ferro-Luzzi, "Proposal for an absolute luminosity determination in colliding beam experiments using vertex detection of beam-gas interactions", Nucl. Instrum. Meth. A **553**, 388 (2005).

[33] G. Anders *et al.*, "LHC bunch current normalization for the October 2010 luminosity calibration measurements", CERN-ATS-Note-2011-016 PERF (2011).

[34] K. Nakamura *et al.*, "Review of particle physics", J. Phys. G **37**, 075021 (2010).